Int. J. of GEOMATE, April, 2016, Vol. 10, No. 2 (Sl. No. 20), pp. 1764-1769
Geotech., Const. Mat. and Env., ISSN: 2186-2982(P), 2186-2990(O), Japan

STABILITY CHARTS FOR A TALL TUNNEL IN UNDRAINED CLAY

Jim Shiau[1], Mathew Sams[1] and Jing Chen[1]
[1]School of Civil Engineering and Surveying, University of Southern Queensland, Australia

ABSTRACT

The stability of a plane strain tall rectangular tunnel in undrained clay is investigated in this paper using shear strength reduction technique. The finite difference program *FLAC* is used to determine the factor of safety for unsupported tall rectangular tunnels. Numerical results are compared with upper and lower bound limit solutions, and the comparison finds a very good agreement with solutions to be within 5% difference. Design charts for tall rectangular tunnels are then presented for a wide range of practical scenarios using dimensionless ratios ~ a similar approach to Taylor's slope stability chart. A number of typical examples are presented to illustrate the potential usefulness for practicing engineers.

Keywords: Stability Analysis, Tall Tunnel, Undrained Clay, Factor of Safety, FLAC, Strength Reduction Method

INTRODUCTION

The critical geotechnical aspects for tunnel design discussed by Peck (1969) in [1] are: stability during construction, ground movements, and the determination of structural forces for the lining design. The focus of this paper is on the design consideration of tunnel stability that was expressed by a stability number initially defined by Broms and Bennermark (1967) [2] in equation 1:

$$N = \frac{\sigma_s - \sigma_t + \gamma H}{S_u} \qquad (1)$$

Where σ_s is the uniform surcharge pressure on the surface and σ_t is the uniform internal tunnel pressure. H is the overburden depth that equals to the sum of cover depth C and half the tunnel height $D/2$. The soil mass surrounding the tall tunnel is assumed as uniform Mohr-Coulomb material with a unit weight (γ) and undrained shear strength (S_u). A schematic diagram of the problem is shown in figure 1.

The stability number presented in equation 1 has been re-defined and approached by the upper and lower bound solutions (Davis et al. 1980 [3]; Sloan et al. 1988, 1989 and 1991 [4, 5, 6]). The problem was regarded as to find the limiting value of an overburden pressure ratio $(\sigma_s - \sigma_t)/S_u$ that is a function of the independent parameters such as the depth ratio C/D and the strength ratio $S_u/\gamma D$. Other similar tunnel stability research such as using pressure relaxation and finite difference methods can be found in Shiau et al. (2013 and 2014) [7, 8].

It is possible to further simplify this stability number by neglecting σ_s and σ_t to simulate an unsupported excavation in green-field conditions. The problem is then reduced to a simpler factor of safety problem that is a function of the depth ratio C/D and the strength ratio $S_u/\gamma D$. This approach is very similar to the widely used Taylor's design chart for slope stability analysis (Taylor, 1937) [9].

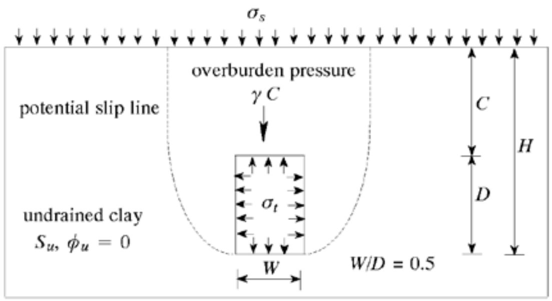

Fig. 1 Statement of the tall tunnel problem ($W/D = 0.5$)

Very little research was carried out on the shape influence of underground tunnels. With the recent advanced development of computational technique, it is possible to design tunnels with different shape such as "tall" tunnels. This paper investigates the stability of a plane strain tall rectangular tunnel in undrained clay. A strength reduction technique is used to determine the factor of safety of tall tunnels in cohesive soils over a wide parametric range in green-field conditions. Results obtained from the strength reduction technique in *FLAC* are compared to those using the finite element limit analysis *FELA*. A series of stability charts using the *FoS* approach is produced for practical applications.

PROBLEM DEFINITION

Tunnelling is a complex three dimensional problem in nature and therefore it is often reduced to a two-dimensional one by assuming the transverse section as a very long tunnel.

As shown in figure 1, the soil body is considered as undrained and modelled as a uniform Tresca material, which is the same as a Mohr-Coulomb material with zero soil friction angle ($\varphi_u = 0$), the non-zero undrained shear strength (S_u), and the saturated unit weight (γ). The dimension of the tall tunnel is ($W * D$) and the cover depth is C. The soil strength ratio (*SR*) is represented by $S_u/\gamma D$. The factor of safety (*FoS)* is used to represent the stability of the tall tunnel that is a function of the depth ratio (*C/D)* and strength ratio ($S_u/\gamma D$) as indicated in equation (2). The definition of a tall tunnel in this paper is for the width-height ratio W/D = 0.5. This ratio has been used to obtain all numerical results throughout this paper.

$$FoS = f\left(\frac{C}{D}, \frac{S_u}{\gamma D}\right) \tag{2}$$

The parameters used in this paper are $S_u/\gamma D = 0.2 - 2$ and $C/D = 1 - 6$, which should cover most of the realistic parameters and ensure that the *FoS* design charts produced can be applicable to many different tunnel design and analysis problems.

FLAC MODELLING TECHNIQUE

The shear strength reduction method is commonly used for slope stability analysis using finite element or finite difference methods. However, this method remains uncommon in tunnel stability analysis. With the advent of powerful computers and simulation programs in recent years, it is gradually being considered as an alternative method for tunnel stability analysis.

A typical finite difference half mesh of the problem, due to the symmetric condition, is shown in figure 2. The boundary conditions shown in the figure are important, they ensure that the entire soil mass is modelled accurately despite using a finite mesh. The soil domain size for each case was selected to be large enough so that the failure zone of soil body is placed well with the domain. Note that the base and sides of the model is restrained in the *x* and *y* directions. For those nodes along the symmetrical line, only the x translation is restrained. This allows vertical translation along the symmetrical plane.

In the shear strength reduction method (*SSRM*), the shear strength of the material is reduced until the limiting condition is found where a factor of safety can be defined. The factor of safety (*FoS*) being studied in this paper are computed by using explicit finite difference code via *FLAC*. Although the code is based on the explicit finite difference method, it is not very different from a nonlinear finite element program. The factor of safety is defined as a ratio of the strength necessary to maintain limiting equilibrium with the soil's available strength. If the material triggers the failure condition initially, then the cohesion and friction angle is increased until limiting equilibrium or failure state is reached. Once the actual and critical strength are known, they are used to calculate the factor of safety (*FoS*).

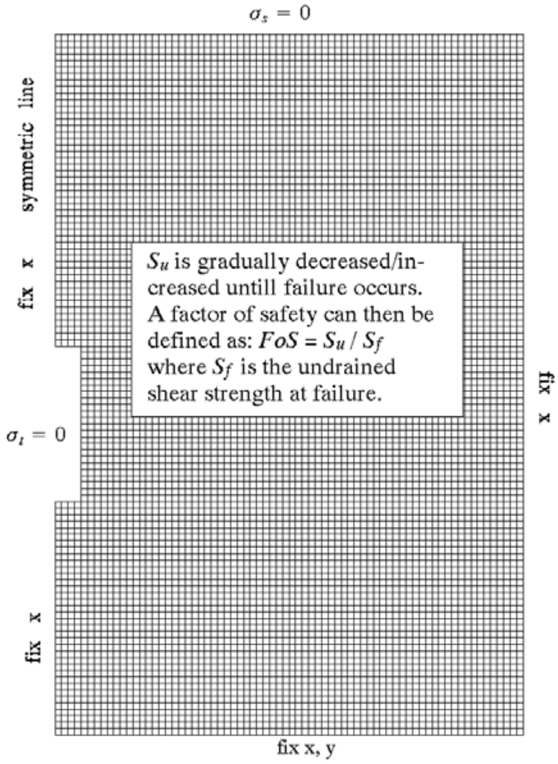

Fig. 2 Typical half mesh and boundary conditions (*W/D* = 0.5)

RESULTS AND DISCUSSION

Using the shear strength reduction method and the finite difference program *FLAC*, the values of factor of safety (*FoS)* were obtained for a range of parameters in undrained clay. This parametric study covered dimensionless parameters, including the depth ratio (*C/D*) and the strength ratio *SR* ($S_u/\gamma D$).

Tables 1 and 2 present the numerical results obtained in this study. Graphical comparisons are also presented in figures 3 - 5. In figure 3, *FoS* increases linearly as the strength ratio $S_u/\gamma D$ increases, indicating that there exists a stability number where the effective *FoS* is equal to one, i.e. a critical strength ratio $(SR)_c$. This could be achieved by dividing *SR* by the *FoS* result for each case i.e. the critical strength ratio $(SR)_c = S_u/(\gamma D FoS)$. Note that the rate of *FoS* increase is different for each *C/D* value. The gradient of the line is less for larger *C/D* values. This indicates that it is more beneficial to increase soil strength in shallow tunnel than in deep tunnel.

Figure 4 shows that the *FoS* decreases nonlinearly with increasing depth ratio *C/D* for all strength ratios defined as $S_u/\gamma D$. It should be noted that the strength ratio is normalised with respect to γD, and the undrained shear strength (S_u) remains constant throughout the increasing depth ratios. When *C/D* increases and the undrained shear strength (S_u) remains constant, the *FoS* values decreases due to the increasing overburden pressure. This is in contrast to the common belief that an increase to *C/D* always results in an increase to *FoS* due to the presence of geometrical arching effect.

Table 1 – *FoS* results *(C/D=1, 2, and 3)*

C/D	$S_u/\gamma D$	*FLAC* (Finite Difference) *SSRM**
1	0.2	0.42
	0.4	0.85
	0.6	1.27
	0.8	1.69
	1.0	2.11
	1.3	2.75
	1.6	3.38
	2	4.22
2	0.2	0.31
	0.4	0.62
	0.6	0.94
	0.8	1.24
	1.0	1.56
	1.3	2.02
	1.6	2.49
	2	3.11
3	0.2	0.26
	0.4	0.51
	0.6	0.76
	0.8	1.02
	1.0	1.28
	1.3	1.65
	1.6	2.04
	2	2.55

** Shear Strength Reduction Method (SSRM)*

A simple observation can be made from figure 1, where the active force (γC) is the weight of soil and the resisting force is given by the shear strength of the soil. Given two hypothetical tunnels in the same cohesive soil but at different depths, the tunnel with the smaller active force will yield a higher factor of safety, and therefore have higher stability. This observation may not be true in a soil with internal friction angle due to the additional shear strength from the second term of the shear strength equation ($\sigma tan\phi$) and the geometrical arching effects. In purely cohesive soils, the latter still occurs, but its effect is not enough to overcome that subsequent increase in active force.

Table 2 – *FoS* results *(C/D=4, 5, and 6)*

C/D	$S_u/\gamma D$	*FLAC* (Finite Difference) *SSRM**
4	0.2	0.23
	0.4	0.46
	0.6	0.69
	0.8	0.92
	1.0	1.15
	1.3	1.49
	1.6	1.84
	2	2.30
5	0.2	0.20
	0.4	0.40
	0.6	0.60
	0.8	0.81
	1.0	1.01
	1.3	1.31
	1.6	1.62
	2	2.02
6	0.2	0.18
	0.4	0.36
	0.6	0.54
	0.8	0.72
	1.0	0.90
	1.3	1.17
	1.6	1.45
	2	1.81

** Shear Strength Reduction Method (SSRM)*

Relying on one single numerical model is imprudent; result verification is required in order to improve the solution confidence. For this purpose, it is important to compare the solutions with rigorous upper bound and lower bounds (Optum G2, 2013) [10]. This comparison is shown in figure 5. The critical strength ratio $(SR)_c = S_u/(\gamma DFoS)$ is presented with various depth ratios *(C/D)*. It is encouraging to see that the finite difference results using shear strength reduction technique are in good agreement with the upper and lower bound solutions.

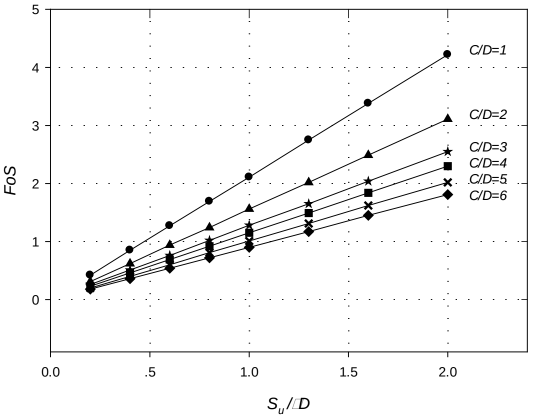

Fig. 3 Comparison of *FoS* results with respect to $S_u/\gamma D$ for various values of *C/D*

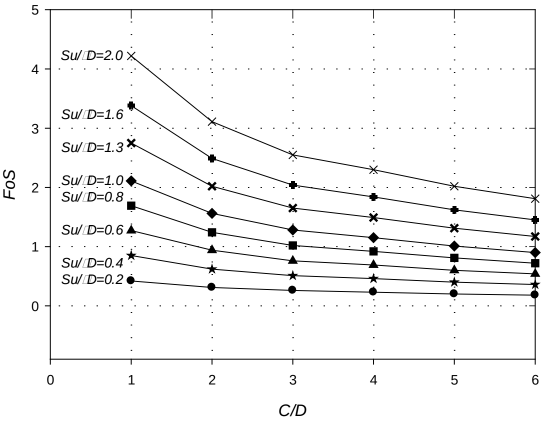

Fig. 4 Comparison of *FoS* results with respect to *C/D* for various values of $S_u/\gamma D$

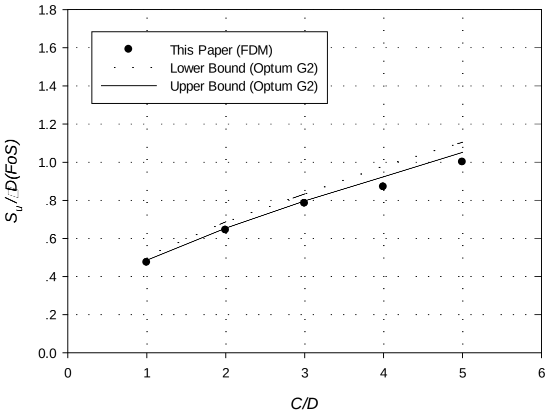

Fig. 5 Comparison of critical strength ratio $(SR)_c = S_u / \gamma D(FoS)$

Figures 6 and 7 show typical plots of the velocity field and shear strain rate. This information of failure extent for various *C/D* values is important as it will assist practising engineers to make a decision in relation to monitoring ground movements. It was noted that the strength ratios, $SR = S_u/\gamma D$, have no impact on the failure extent. This can be understood by observing the linear relationship (constant gradient) between *FoS* and $S_u/\gamma D$ in figure 3.

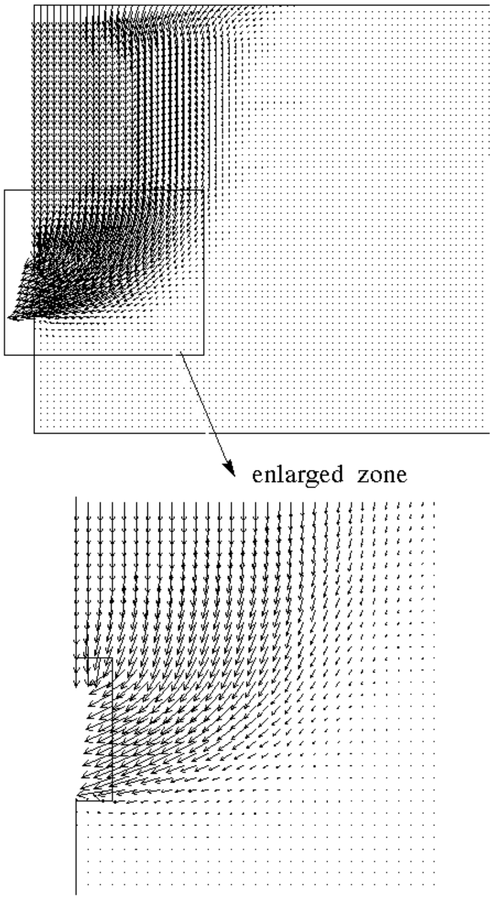

Fig. 6 Plot of velocity field for *C/D*=3.0 and $S_u/\gamma D$ = 1.0

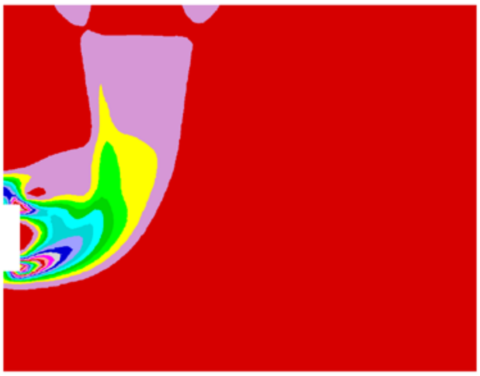

Fig. 7 Plot of shear strain rate showing the potential slip surface (*C/D*=3.0 and $S_u/\gamma D$ = 1.0)

Figure 8 shows a typical principal stress tensor plot that is normally used to study the potential effects of arching phenomenon. This plot shows the directions of major and minor principal stresses, indicating weak soil arching throughout the soil body. As discussed, soils with an internal friction angle ($\phi \neq 0$) would have more potential for stability, with the internal frictional angle adding to the strength of the material by the soil arch (major principal stress rotation).

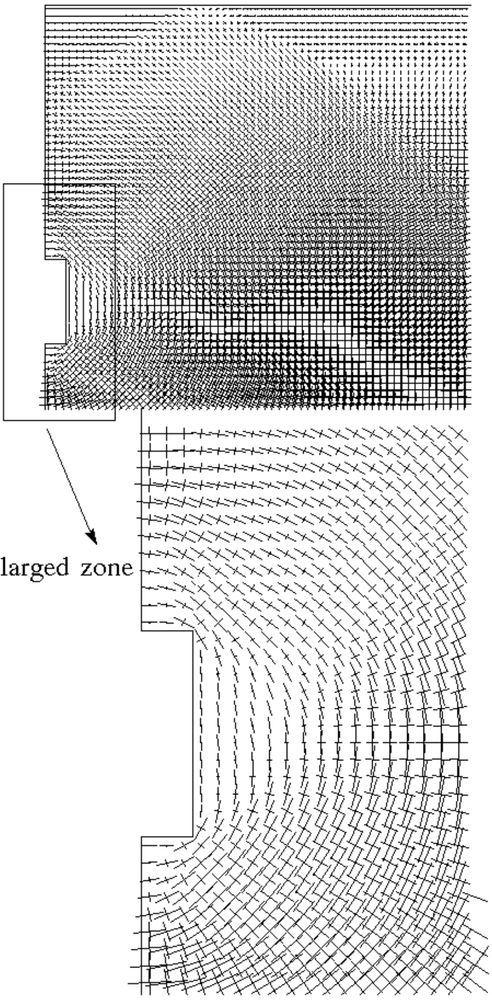

Fig. 8 Principle stress tensor plot at collapse for *C/D* = 3.0 and $S_u/\gamma D$ = 1.0

THE STABILITY CHART

The stability design chart is best demonstrated through a number of examples. Using the numerical results presented in Tables 1 and 2, a contour design chart for *FoS* has been produced in figure 9 that can be used by tunnel engineers to relate the depth ratio (*C/D*), soil strength ratio ($S_u/\gamma D$) and factor of safety (*FoS*). Regression of the design chart gives the following relationship (equation 3) with $r^2 = 0.997$.

$$FoS = 2.133\left(\frac{S_u}{\gamma D}\right)\left(\frac{C}{D}\right)^{-0.466} \quad (3)$$

Using the design chart (figure 9) and equation (3), the following practical examples are illustrated for either analysis or design purposes.

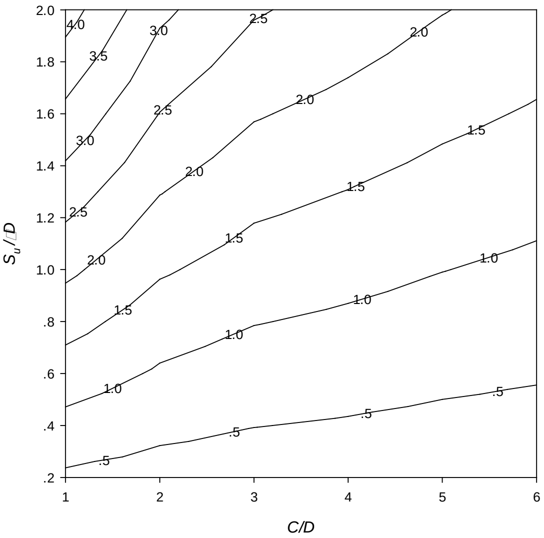

Figure 9 Stability chart for *FoS* with respect to *C/D* and $S_u/\gamma D$

Analysis of an existing unsupported tall tunnel

For an existing unsupported square tunnel without surcharge load (σ_s) and capacity to provide internal supporting pressure (σ_t), determine the factor of safety of the tunnel given the parameters S_u = 86.40 kPa, γ = 18 kN/m^3, *C* = 18 m, and *D* = 6 m.

1. Using *C/D* = 3.0, $S_u/\gamma D$ = 0.8, equation 3 gives a *FoS* of 1.02.
2. Using *C/D* = 3.0, $S_u/\gamma D$ = 0.8, Figure 9 gives an approximate *FoS* of 1.04.

An actual computer analysis of this particular case gives a *FoS* of 1.02.

Design of an unsupported tall tunnel

The soil properties are known at the tunnel project site, and the dimension is specified. A target factor of safety is chosen, and the designers need to specify a maximum cover depth that will satisfy the target *FoS*. Parameters are given as: S_u = 108 kPa, γ = 18 kN/m^3, *D* = 6m, and the target *FoS* = 1.5

1. Using *FoS* = 1.5 and $S_u/\gamma D$ = 1.0, equation 3 gives a *C* value of 12.78 m (*C/D* = 2.13).

2. Using *FoS* =1.5 and $S_u/\gamma D$ = 1.0, Figure 9 gives an approximate *C/D* value of 2.2 and therefore *C* value of 13.2 m.

An actual computer analysis for this particular case (*C* value of 13.2m) gives a *FoS* of 1.48.

CONCLUSION

Stability of plane strain tall tunnels was investigated in this paper by using the shear strength reduction technique and the finite difference *FLAC* modelling. Numerical results of factor of safety (*FoS*) were in good agreement with rigorous upper and lower bound limit analysis. Design charts and equation were produced and illustrated examples presented. The study has concluded that the factor of safety approach to tunnel stability provides an alternative option for the designer and is useful to provide direct information and understanding of tunnel stability. It is recommended that further research be undertaken in relation to non-zero pressure ratios considering the effect of surcharge pressure.

REFERENCES

[1] Peck RB (1969). 'Deep excavations and tunneling in soft ground', *Proceedings of 7th International Conference on Soil Mechanics and Foundation Engineering*, Mexico City. Mexico, pp. 225-298.

[2] Broms BB, Bennermark H (1967). 'Stability of clay at vertical openings', *Journal of the Soil Mechanic & Foundations Division*, Proceedings of the American Society of Civil Engineers, vol. 93, pp. 71- 93.

[3] Davis EH, Gunn MJ, Mair RJ, Seneviratne, HN (1980). 'The stability of shallow tunnels and underground openings in cohesive material', *Geotechnique*, vol. 30, pp. 397-416.

[4] Sloan, SW (1988). 'Lower bound limit analysis using finite elements & linear programming', *International Journal for Numerical & Analytical Methods in Geomechanics*, vol. 12, pp. 61-67.

[5] Sloan SW (1989), 'Upper bound limit analysis using finite elements & linear programming', *International Journal for Numerical & Analytical Methods in Geomechanics*, vol. 13, pp. 263-282.

[6] Sloan SW, Assadi A (1991). 'Undrained stability of a square tunnel in a soil whose strength increases linearly with depth', *Computers and Geotechnics*, 12, pp. 321-346.

[7] Shiau, JS, Kemp RJ (2013). 'Developing a numerical model for the stability design of tunnel heading', *Third International Conference on Geotechnique, Construction Materials & Environment*, Nagoya, Japan.

[8] Shiau JS, Sams MS, Zhang J, Kemp RJ (2014). 'Settlement analyses of underground circular tunneling in soft clay', *Geotechnical aspects of underground construction in soft ground*. Taylor & Francis (CRC Press) / Balkema, Leiden, Netherlands, pp. 347-352.

[9] Taylor DW (1937). 'Stability of earth slopes' *Journal of the Boston Society of Civil Engineers*, vol. 24, no. 3, pp. 197-246.

[10] Optum G2 (2013), Optum Computational Engineering, Version 1.2014.10.1, Newcastle, Australia.

[11] *FLAC* 2003, Fast Lagrangian Analysis of Continua, Version 4.0, Itasca Consulting Group, Minneapolis, Minnesota, USA.

Int. J. of GEOMATE, April, 2016, Vol. 10, No. 2 (Sl. No. 20), pp. 1764-1769.
MS No. 09714 received on Oct. 09, 2015 and reviewed under GEOMATE publication policies.

Pertinent discussion including authors' closure, if any, will be published in Dec. 2016 if the discussion is received by June 2016.
Corresponding Author: Jim Shiau